



VICTORIA UNIVERSITY
MELBOURNE AUSTRALIA

The relevance of large-scale battery energy storage (BES) application in providing primary frequency control with increased wind energy penetration

This is the Accepted version of the following publication

Datta, Ujjwal, Kalam, Akhtar and Shi, Juan (2019) The relevance of large-scale battery energy storage (BES) application in providing primary frequency control with increased wind energy penetration. *Journal of Energy Storage*, 23. pp. 9-18. ISSN 2352-152X

The publisher's official version can be found at
<https://www.sciencedirect.com/science/article/pii/S2352152X1830759X>
Note that access to this version may require subscription.

Downloaded from VU Research Repository <https://vuir.vu.edu.au/38265/>

The relevance of large-scale Battery Energy Storage (BES) application in providing primary frequency control with increased wind energy penetration

Ujjwal Datta^{a,*}, Akhtar Kalam^a, Juan Shi^a

^aCollege of Engineering and Science, Victoria University, P.O. Box 14428, Victoria 8001, Melbourne, Australia

Abstract

Renewable energy sources (RES) based distributed generation (DG) system results reduction of overall system inertia, which is likely to generate higher oscillations in the system during disturbance conditions. Therefore, DG penetration level has a significant impact on system stability and reliability. This study provides an in-depth analysis of Battery Energy Storage System (BESS) impact in providing primary frequency control to support increased wind penetration level. The BESS is modeled as a storage system with DC/AC converter and other associated power electronics interfaces. The objective is to replace the existing synchronous generator in proportion with the increasing penetration level of wind units while maintaining power system stability and reliability. The BESS model is developed in DigSILENT/PowerFactory and the system performances are simulated and compared with and without the BESS considering different disturbances such as single-phase-to-ground fault, and temporary line outage and load demand increment with various DG penetration level. It is shown through simulation results that BESS exhibits the ability to reduce system oscillations following disturbances and supports the increment of DG penetration level in the existing power system. Therefore, BESS can be seen the most viable measure of stability enhancement with renewable oriented sustainable future electric grid.

Keywords: Battery energy storage system, wind penetration, transient stability, frequency oscillations.

1. Introduction

Global concerns on greenhouse gas emission, incentives and code of practice set by governments have results an upward trend in the penetration level of distributed generation (DG) mainly from renewable energy sources (RES) [1]. However, RES comes with a few inherent drawbacks such as its mere dependency on weather condition to generate electricity and its lack of inertia to damp the system oscillation. With an increased amount of intermittent RES, the power system planning and operation is becoming more complex and difficult to ensure the reliability of the network. Wind energy source is one of the most popular forms of RES in present-day power system. The dynamic response of the wind integrated power system is greatly affected by the type of wind generators connected to the system. Among several types of generators, doubly fed induction generator (DFIG) based wind farm has been widely installed due to their cost-benefit and flexibility of regulating the output power [2]. With different dynamics and operational features than synchronous generators, penetration of wind farms may affect adversely on damping out power system oscillation resulting from the curtailment of available system inertia by shutting down synchronous generator based conventional generating units [3]. The foremost technical challenges with DG penetration

are on system stability. Since RES are reducing system inertia, the system may not be able to compensate frequency oscillations within the allowable limit in the presence of a disturbance. Therefore, the necessity of system inertial response is demanding. Based on system inertial response capability, many research efforts have been put to investigate the impact of DG penetration and their limits on the existing system following different dynamic and transient phenomena [4-6]. In near future, the wind farm may be required to participate in certain level of frequency regulation with major DG penetration level. Substantial research efforts is dedicated to improve the frequency regulation and frequency response of wind farm by using rotating mass of wind turbine [7, 8], power and torque droop control [9], optimal dispatch [10], power oscillation damper [11], pitch-angle control for deloading and droop control [12-14] However, such control techniques require the adjustment of power extraction from the wind farm [15-17] which is not desirable by wind farm owner as this will affect wind farm revenue. It is worth mention that, dispatchable energy source based on synchronous generator has been used to restore system frequency. In order to drive for 100% RES, complete dependency on wind farm frequency regulation is not fully reliable as the technology itself is dependent on weather condition. Therefore, dispatchable and reliable alternative energy source is required to ensure the stability of the system with an increased penetration level of wind and other RES in the existing power system. Battery energy storage system (BESS) is an essential and broadly studied alternative to support frequency stability challenges

*Corresponding author at: College of Engineering and Science, Victoria University, P.O. Box 14428, Victoria 8001, Melbourne, Australia. Tel.: +61 0470396067

Email address: ujjwal.datta@live.vu.edu.au (Ujjwal Datta)

related to fluctuating and intermittent RES [18]. Since BESS offers fast active power response, BESS is a perfect choice to compensate for the negative impacts of DGs by reducing oscillations of the power system. It has been shown that the application of BESS significantly improves the transient stability response in a microgrid [19] in an increased DG penetration environment [20]. BESS can improve and affect positively in reducing rotor speed deviation at different DG penetration levels following disturbances in the system [21, 22]. The impact of different BESS operation strategies are investigated in [23] for providing primary frequency control. On the contrary, the authors in [24] demonstrated that BESS significantly reduces environmental impacts while providing primary control. However, earlier works with energy storage system overlooked the ability of BESS to reduce frequency oscillation and increase DG penetration level in the existing system.

Considering aforementioned works, this study presents the contribution of BESS in supporting increased DG penetration level in the existing power system. The objective is to maintain system frequency within a restricted boundary of $\pm 1\%$ of nominal value to comply with power quality standards according to the Australian National Electricity Market [25]. In particular, the main interest of this work is to monitor transient stability phenomena with RES penetration in the electrical grid. This approach is of specific interest of future large-scale RES integrated power system in which the system would be susceptible to power oscillation due to lower system inertia. This technique is able to obtain more information on system inertia reduction with the replacement of the existing synchronous generator (SG) unit by RES unit. In addition, the important role of BESS power and energy is also explored in this study. The impact and the improvement of system inertia by using rapid responsive BESS to facilitate the increased DG penetration level will be investigated through multiple case studies.

2. DG penetration and system inertia

The main technical concern with RES based DG is its reduced inertia as it significantly affects system stability in the case of power imbalances in the system. DG penetration level is defined by the following expression [26]:

$$\%DG = \frac{\sum P_{DG}}{\sum P_{DG} + \sum P_{SG}} \quad (1)$$

where, P_{DG} and P_{SG} are the total active power output from SG and DG units. There are two major aspects that define the severity of DG penetration level and its impact on the overall system inertia. These are detailed as follows:

- Existing SGs remain connected to the system with the increased DG penetration.
- Existing SGs are permanently shut down with the increased DG penetration.

Considering sustainability concern, the existing thermal SG unit based on fossil fuel i.e. coal could be shut down permanently with the increased DG penetration level (whereas small-hydro, biomass, geothermal etc. will remain in operation) in future sustainable energy market. In this study, the replacement of existing SG is considered with the increased penetration level of DG unit. The idea is to incorporate more RES in the grid and increasing the RES penetration level by means of using BESS. The BESS is equipped with bidirectional DC/AC converter and can be controlled to release or absorb energy. Grid frequency and power system oscillation support can be provided by controlling P_{BESS} to regulate grid power according to the operational requirements. The primary focus of this study is to reduce frequency oscillation under disturbance conditions with increased DG penetration level.

To provide inertial control, the required power reference of BESS converter is adjusted according to the capability of the system to respond and can be simplified as follows [27]:

$$P_{ref-1} = P_{ref-0} - H_V f_{nom} \frac{df}{dt} \quad (2)$$

where P_{ref-1} and P_{ref-0} are power reference with and without frequency control, H_V is the inertia constant that defines BESS capability to respond in providing frequency control, f_{nom} is the nominal system frequency (pu) and df/dt is the rate-of-change-of-frequency (pu/s) following any contingency. Primary frequency control has to be activated within a very short time and for a small period of time. Traditionally fossil fuel power plants deliver such frequency control. However, closing down of conventional power plants with increased penetration of renewable energy introduces stability threat in power system. Therefore, BESS is designed to provide primary frequency control with respect to the changes in system frequency via the droop control method. To provide frequency control through droop method, BESS power is adjusted as follows:

$$P_{ref-1} = P_{ref-0} + K_R df \quad (3)$$

where, K_R is the droop gain of BESS and df is the frequency deviation. However, the authors in [28] presented that droop control demonstrates better power regulation than inertia control. Hence, in this paper, BESS is designed to provide frequency response with respect to the changes in system frequency via droop control method. The maximum deviation of system frequency is controlled by regulating the primary frequency control gain i.e. droop gain ($1/R$) where R is the droop value. In addition to droop value, parameters of other controllers such as BESS converter rating, PI controller parameters also play significant roles in controlling the frequency response and regulating system oscillations.

3. The control diagram of Battery energy storage system (BESS)

BESS mainly provides frequency oscillation damping by absorbing excess power and supplying shortfall of power. The

basic BESS structure consists of a battery bank, bidirectional DC/AC converter and a grid connected transformer. The detail control technique of BESS is shown in Fig. 1. There are mainly 5 individual control sections in BESS control:

- Frequency controller
- Voltage controller
- Active Power (P) and Reactive Power (Q) control
- Charge controller
- Current controller on direct (d) and quadrature (q) axis

3.1. Frequency controller

The frequency controller takes action when the grid frequency differs from nominal value as per expression in (4)

$$df = f_{ref} - f_{grid} \quad (4)$$

BESS absorbs energy (charging) if df is negative and supplies energy (discharging) if df is positive. The deadband is included to avoid BESS operation during a small change in the frequency and to comply with the grid code. The droop sets the limits of the battery full active power activation in response to a certain amount of frequency deviation from the nominal value as per the following expression in (5)

$$P_{BESS} = \pm df / droop(R) \quad (5)$$

3.2. Voltage controller

The voltage controller takes action when the grid voltage differs from the nominal value as per expression in (6)

$$dv = V_{ref} - V_{bus} \quad (6)$$

BESS absorbs reactive power if dv is negative and provides reactive power if dv is positive. The droop sets the limits of battery full reactive power activation in response to a certain amount of voltage deviation from the nominal value as per the following expression in (7)

$$Q_{BESS} = \pm dv / droop(R) \quad (7)$$

3.3. Active Power (P) and Reactive Power (Q) control

In PQ control, the active and reactive power at BESS output terminal P_{in} and Q_{in} are compared against incoming active and reactive power reference from the frequency and voltage controller. The signal Δi_d which is the difference between the charge controller input and the output current on the d-axis is added with active power difference and then a PI controller is used to generate the active current reference on the d-axis. The deviation between the reference voltage value and the voltage at BESS connection point is used as an input to another PI controller to generate reactive current reference on the q-axis. The difference between the charge controller input and the output current on the q-axis Δi_q is added with reactive power difference in PQ controller. However, since the main purpose of this study is to acquire frequency oscillation support, the active power is given preferences over reactive

power via deadband and lower gain for reactive power activation. A first order low pass filter is used to smooth out the input. Time constant in low pass filter defines the dynamic behavior of the output with respect to the input. Thus a large time constant value results large energy storing component that causes slower change in transient response. To avoid integrator windup, PI controller with an anti-windup limiter is used. The PI controller is described by Fig. 2 where x_i can be expressed by the following expression:

$$x_i = K_i / T_i \quad (8)$$

where $y_o = i_{d-ref}$, $y_{min} = i_{d-min}$ and $y_{max} = i_{d-max}$ for d-axis and $y_o = i_{q-ref}$, $y_{min} = i_{q-min}$ and $y_{max} = i_{q-max}$ for q axis.

The PI controller representation can be calculated as:

$$y_o = \left(K_p * y_i + \frac{K_i}{T_i} \int_{y_{min}}^{y_{max}} y_i dt \right) \quad (9)$$

The controller is bounded by the maximum and minimum value and the parameters are tuned by trial and error method to reduce the frequency undershoot (f_{nadir}), frequency overshoot (f_{max}) and settling time (t_{st}). Although the maximum rate of change of power (ROCOP) is not implemented in this study, a rate limiter can be added at the active power current reference output to control ROCOP value. The corresponding PI parameters are given in Appendix A.

3.4. Charge controller

Charge controller generates a charging/discharging signal based on the available state-of-charge of the battery and incoming current reference value of d-axis. The BESS regulates the active power if battery SOC satisfies the defined operating conditions. The SOC conditions are outlined in (10). Since reactive power is not dependent on battery, reactive current is not considered in charge control. However, current limiter restricts total amount of current flow through d and q-axis within the design limits to avoid over-loading of BESS converter. Hence, total current would be the maximum absolute value of 1. The SOC control and the charge controller parameters are outlined in Appendix A. The SOC control in the charge controller is delimited as follows:

$$i_{d-in} = \begin{cases} i_{d-ref} & SOC_{min} \leq SOC \leq SOC_{max} \\ 0 & otherwise \end{cases} \quad (10)$$

The battery can be charged when the frequency is within the grid defined deadband region. Battery can be charged if SOC is less/equal than SOC_{max} and discharged if SOC is greater/equal than SOC_{min} . Battery cannot be charged if SOC is greater than SOC_{max} and discharged if SOC is lower than SOC_{min} . The current limiter regulates the active and reactive power output reference within the total BESS converter capacity. The active power reference regulates within the maximum BESS converter capacity ($\pm 1 pu$). Based on the

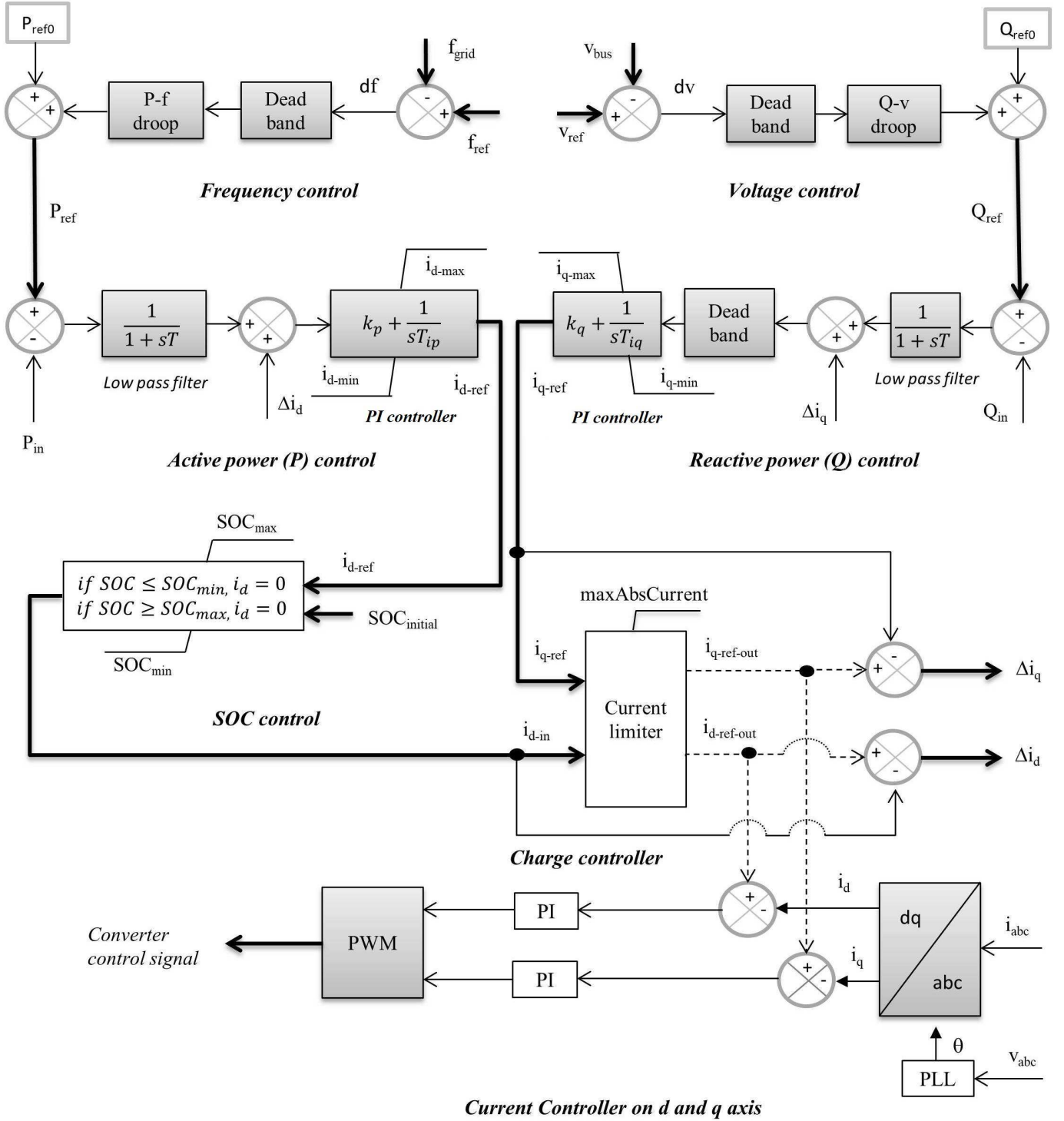


Fig. 1 The detailed BESS control techniques

remaining BESS converter capacity, the reactive power output reference is executed i.e. within $\pm Y$, where Y varies between 0 to 1 and can be calculated as in (11):

$$Y = \sqrt{1 - (i_{d-ref-out}^2)} \quad (11)$$

The maximum and minimum BESS converter value can be

adjusted individually for the positive and negative current.

3.5. dq current controller

The input to the current controller is the AC current at BESS converter output in dq reference frame. Phase-locked-loop (PLL) is used to synchronize BESS with the grid. PI controller regulates d and q-axis currents to

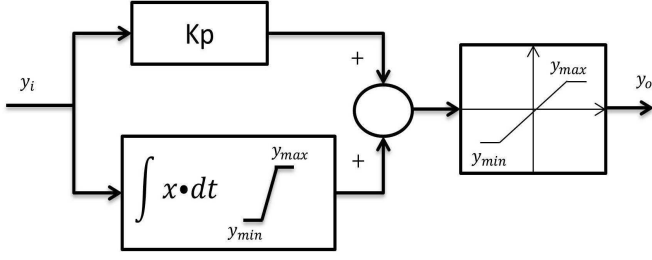


Fig. 2 Block diagram of PI controller with anti-windup

regulate active and reactive power. The pulse width modulation (phase and magnitude) is defined by the modulation index on d and q axis, with reference to the reference system defined by cosine and sin. The PI parameters are given in Appendix A. The PI controller in the current controller is expressed as:

$$K_p + K_i/(sT_{ip}) \quad (12)$$

3.6. Effect of Charge/Discharge on Battery Lifetime

Among multiple factors, battery charge/discharge cycling which is defined as depth-of-discharge (DOD) is one of the main factors that degrade battery lifetime [29]. With a charging/discharging battery current of I_{batt} , the DOD can be calculated by (13) [30]

$$DOD(t) = DOD(t_o) + \frac{I_{batt} \Delta t}{C_R} 100\% \quad (13)$$

where, Δt is the difference in operating period, C_R is the rated BESS capacity. The higher charging/discharging current increases the change in DOD over the operating period and thus impacts negatively on battery lifetime. Battery lifetime L_{Batt} can be calculated by (14) [31]:

$$L_{Batt} = \frac{1}{\sum_{n=1}^N \frac{NC_n}{CFd_n}} \quad (14)$$

where, NC_n is the number of cycles at a DOD, CFd_n is the cycles to failure at a DOD, $n=1$ to N is the DOD ranges. Hence, it can be seen from (14) that battery lifetime is negatively affected by cycles with higher DOD than the lower DOD. Fast charging/discharging cycles in frequency control will reduce the lifetime of a battery. Nevertheless, estimation of battery lifetime is not the focus of this paper, but interested readers can find suitable information on battery lifetime calculation in [32, 33].

3.7. Battery Model

The selected battery model in this study is a simple R_{int} equivalent model which is widely used in the past [32, 33] and shown in Fig. 3.

The battery is modeled as a SOC dependent voltage source with internal resistance (R_{int}) and can be calculated as in (15) [34]:

$$U_{DC} = U_{max} SOC + U_{min}(1 - SOC) - I_{batt} R_{int} \quad (15)$$

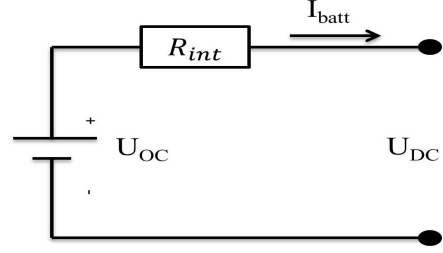


Fig. 3 Block diagram of R_{int} equivalent battery model

4. System modeling and Case Studies

The studied system and the case studies are discussed in this section.

4.1. System modeling

The power system used in this study is an IEEE 9 buses, 3 synchronous generators (SGs) system as shown in Fig. 1 [35]. For this study, all the generators are equipped with an exciter, AVR and G2 is modelled as Gas turbine, G1 as hydro governor and G3 as Coal power plant with associated governor and IEEE Type AC1 Excitation System. The detail information of the exciter and governor models can be found in [36]. G1 is considered as reference machine. This study is conducted in DigSILENT /PowerFactory.

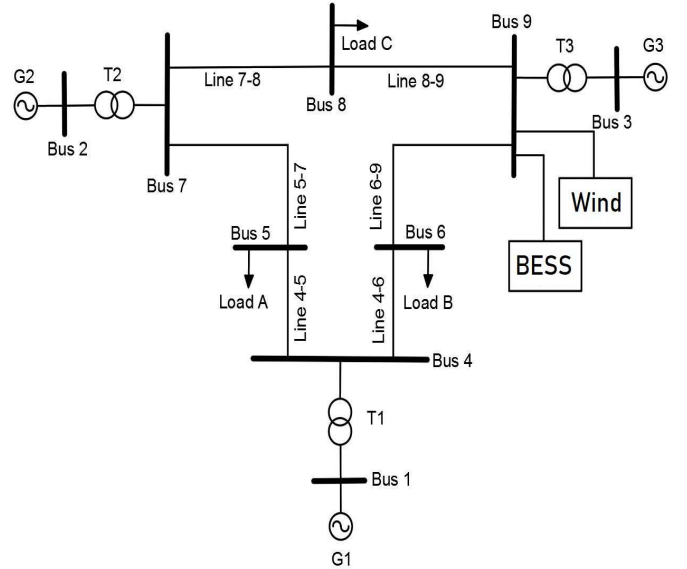


Fig. 4 Block diagram of power system with the installed DG

The aggregated wind farm unit is installed at bus 9 via a 0.69/230kV transformer and the 40 MW BESS is installed via a 0.4/230kV transformer. Each wind turbine is rated as 2.2 MW. Doubly fed induction generation (DFIG) based generator is used for a wind farm and DFIG is designed with fault-ride through (FRT) capability. The detail information of the DFIG model can be found in [37]. The total active power demand of the system is 315 MW. The nominal apparent power for G1 and G2 are 250 MVA and 300 MVA with the power factor of 1.

To analyse the impact of the maximum wind penetration level, it is considered that the wind farm is operating at its maximum rated output according to the wind speed vs power output curve as shown in Fig. 2 i.e. the wind speed is between 15-25 m/s at the time of transient fault analysis. However, when the wind farm operates below the rated wind speed, the output power of the wind farm will be lower than the maximum penetration limit. Therefore at lower wind penetration level, the system frequency does not oscillate beyond the specified grid constraints.

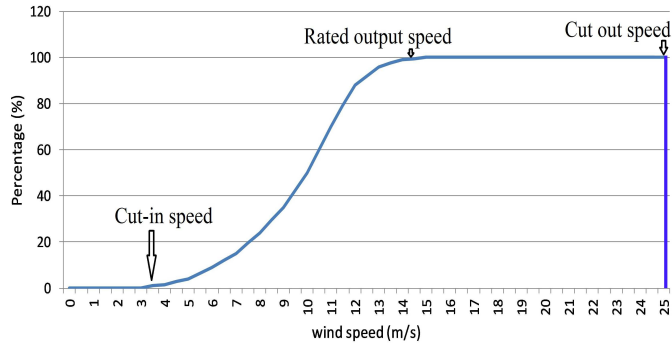


Fig. 5 Wind farm output power as percentage of rated capacity with varying wind speed

4.2. Case Studies

DG penetration level and its impact on the power system always depend on the nature of the type and the installation location of DG, as well as the type and location of the faults. In order to gain an understanding of DG penetration, three different types of case studies are investigated.

- *Case-1:* Single phase to ground fault.
- *Case-2:* Heavy loaded line outage during a fault.
- *Case-3:* Load event

Based on different scenarios, frequency operation limit is checked. The impact of DG units is studied depending on four different states of affairs:

- Without any wind power penetration.
- Wind penetration limit with the removal of G3 unit.
- Higher level wind penetration without BESS incorporation.
- Higher level of wind penetration with BESS incorporation.

5. Result and analysis

To verify the effectiveness of BESS in reducing oscillation and supporting increased DG penetration, simulation investigations have been carried out in DigSILENT/PowerFactory. The target is to replace existing G3 generator and install wind farm of equal rating. The limit of wind farm penetration level is identified when SG unit is replaced by the wind farm. Wind farm is connected to bus 9.

For this case study, the wind farm is operating at its maximum capacity and producing the equal power of G3 unit. However, the different power output of wind farm is used in case of identifying wind energy penetration limit following various types of disturbances. Considering FRT requirement by the grid, wind farm is expected to be remaining connected during the fault and provides output right after the fault clearance. In this study, wind farm is not designed to provide damping of oscillations. Reference synchronous machine G1 is considered to provide the primary frequency bias of 20MW/Hz in response to actual system frequency deviation for all simulation case studies and conditions.

5.1. Case study-1: DG penetration and single-phase-ground fault

During a transient fault in the system, the inertial capability to support system damping is investigated with different penetration level of wind; with and without BESS. A 150 ms (0-0.15s) single-phase-to-ground (phase-a) fault is applied at bus 6. In the case of higher wind penetration level when G3 unit is shut down permanently, the system oscillation increases as system inertia decreases with the removal of G3. Fig. 6 illustrate the frequency for G2 during single-phase-to-ground fault. It can be seen that with 92 MW wind power i.e. 14.33% is the penetration, minimum and maximum frequency oscillations stay within the limit without the integration of battery storage system.

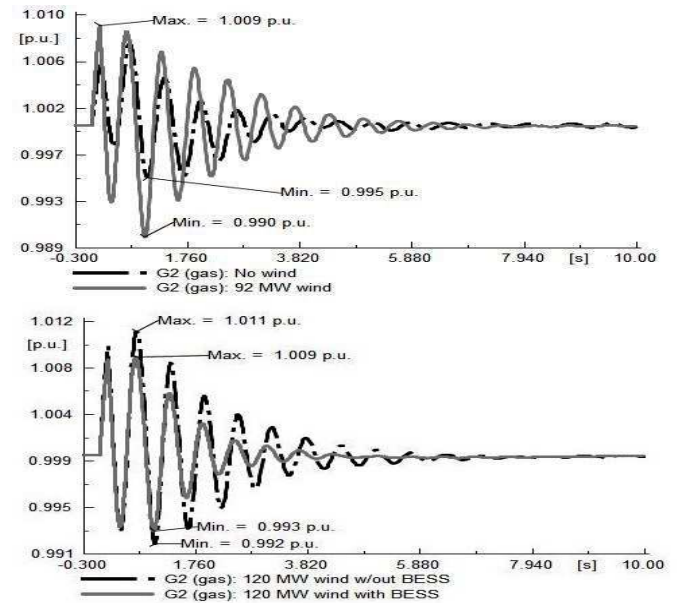


Fig. 6 Frequency of generator G2 with single-phase-ground fault (phase-a)

Also, the frequency of generator G1 is shown in Fig. 7 that exhibits similar grid satisfactory frequency performance. However, as the objective of this study is to increase wind penetration level, hence, wind power output is increased to 120 MW.

Fig. 6 also shows that with 120 MW i.e. 17.91% wind power output, frequency oscillates beyond the grid defined

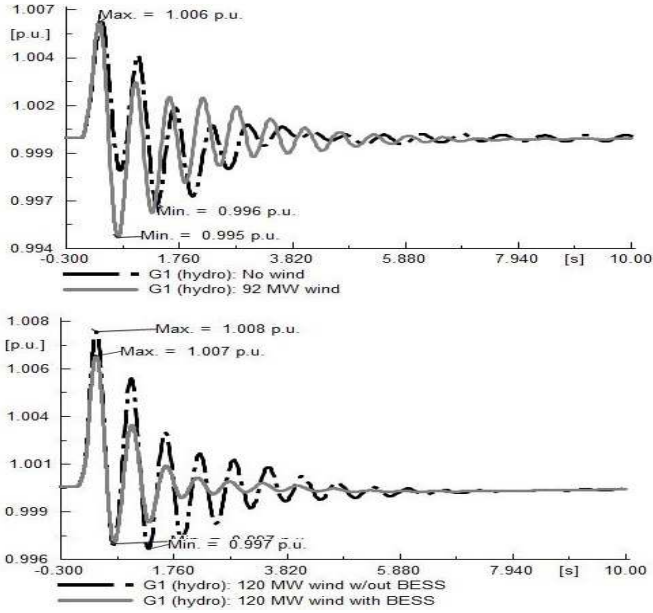


Fig. 7 Frequency of generator G1 with single-phase-ground fault (phase-a)

$\pm 1\%$ of nominal value. However, with the incorporation of BESS, frequency oscillation stays within the operating limit. Hence, it can be seen that BESS integration supports increment in wind penetration level by 3.58%. BESS also reduce deviation in frequency oscillation with respect to the system without BESS. A similar level of reduction in frequency oscillation is visible for G1 as shown in Fig. 7. It is worth noting that the grid has sufficient capacity to deal with the after contingency effect, nevertheless, satisfying grid codes for a short period is not often possible due to the reduced inertia of the system. Such situation insists the urgency of quick responsive alternative measure and BESS has shown its competence in such urgency.

Moreover, BESS also reduces power oscillation following the fault compare to wind penetration without BESS as shown in Figs. 8 and 9. Also, BESS is able to stabilize the system faster than a system without BESS as shown in Figs. 8 and 9.

The maximum power oscillation of G2 reaches 240 MW and a minimum value to 42.9 MW with 120 MW wind power and no integrated BESS. On the other hand, the maximum power oscillation of G1 reaches to a value of 180.7 MW and minimum power oscillation to -57.7 MW with 120 MW wind power and no integrated BESS. But with an incorporated BESS, oscillation of G1 reduces to 156.9 MW (maximum) and -42.2 MW (minimum). Also, the oscillation of G2 reduces to 237.1 MW (maximum) and 57.9 MW (minimum) with the incorporated BESS. Therefore, BESS supports to reduce the deviation in power oscillation. BESS output power is shown in Fig. 10. The maximum active power is approximately 38MW and becomes zero once system frequency restores to the nominal value with the specified deadband region. It can be seen that the amount of reactive power is nearly zero as active power is preferred for primary frequency control. Battery SOC is shown in Fig. 11 that remains nearly the same as the

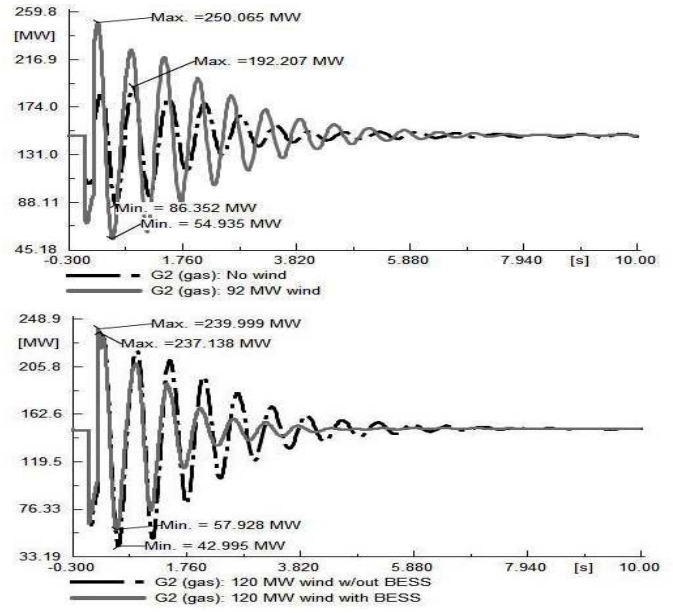


Fig. 8 Active power output of generator G2 with single-phase-ground fault (phase-a)

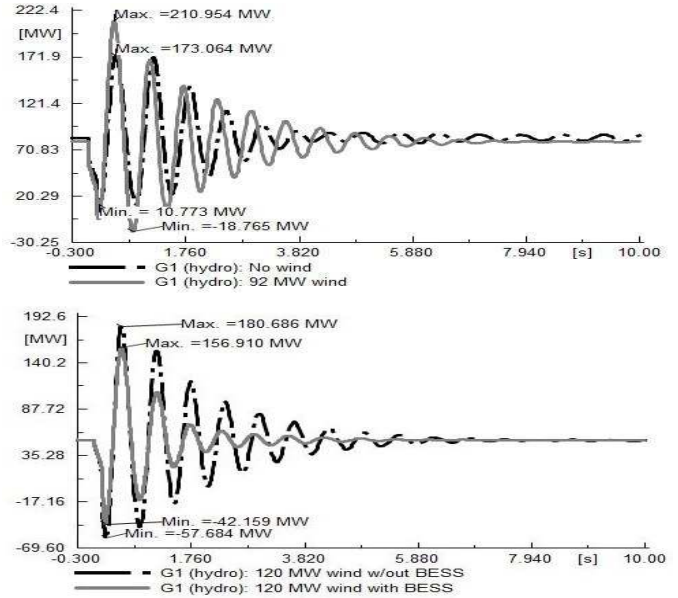


Fig. 9 Active power output of generator G1 with single-phase-ground fault (phase-a)

beginning of the transient event that depicts the need for low energy but high power battery for primary frequency control.

5.2. Case study-2: DG penetration and line 5-7 outage during three-phase fault

Line outage is one of the common disturbances that power system encounters in their daily operation mainly from fallen trees or broken structures. The most heavily line *Line 5-7* outage impact is investigated on DG penetration level. A 240 ms (0-0.24s) duration of line fault is considered in this case. The line is restored after the clearance of fault.

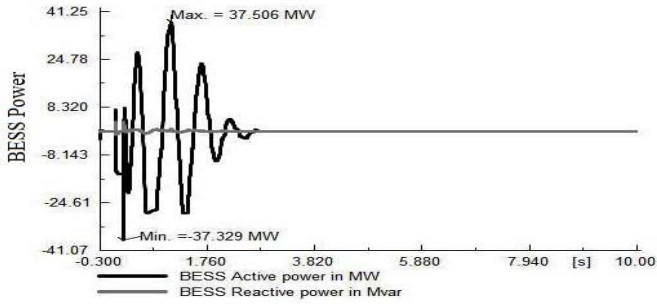


Fig. 10 BESS active/reactive power

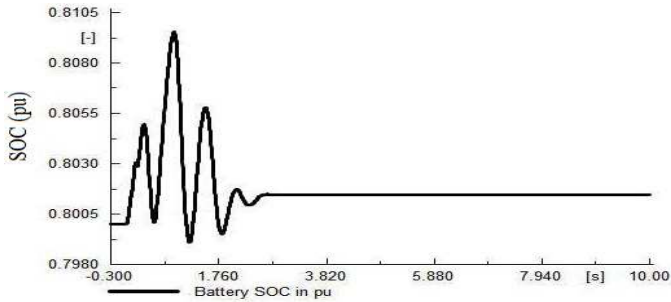


Fig. 11 Battery SOC

Simulation results of line fault are shown in Fig. 12. Following a line fault disturbance, 80 MW i.e 12.7% wind penetration is the limit to keep frequency oscillation within operational boundary as shown in Fig. 12. With 120 MW i.e 17.91% wind power penetration and without BESS, the frequency of generator G2 fluctuates beyond allowable operational boundary as shown in Fig. 12. However, with the integrated BESS generator G2 oscillates within the grid defined acceptable operational periphery, in the case of line fault incident. It can be concluded that BESS facilitates 5.21% increased wind penetration following a line fault.

Simulation results in Figs. 13 and 14 show that BESS reduces active power oscillation considerably compared to increased wind penetration without a BESS. With 17.91% wind penetration and without a BESS, maximum and minimum active powers during oscillations of G1 are 190.2 MW and -71.8 MW. For the same case, maximum and minimum active power oscillations of G2 are 261 MW and 32.3 MW. Nevertheless, when BESS is used with the same level of wind penetration, the oscillations of G1 are 144.3 MW (maximum) and -49.4 MW (minimum). For G2, oscillations are 253.6 MW (maximum) and 62.8 MW (minimum). The above observation clearly announces the efficacy of BESS in enhancing primary frequency control stability with increased penetration of low inertia wind energy sources.

BESS output power is shown in Fig. 15. BESS reduces oscillations by absorbing excess energy and supplying energy shortfall, resulting from contingency events. As the minimum d-axis and q-axis value is selected as -0.7pu (as given in Appendix A), BESS power consumption is -70% of the rated BESS capacity i.e. 28MW of the 40MW rated capacity. This value can be selected as 1pu to use the total BESS capacity.

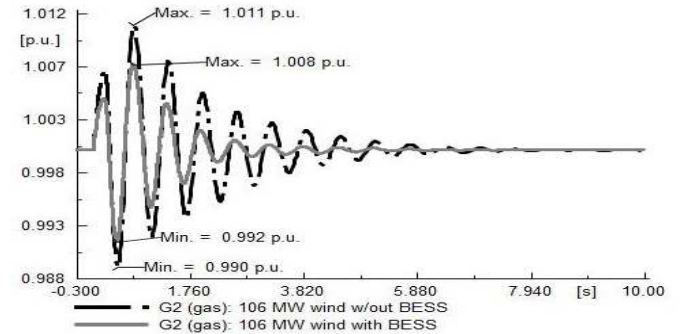
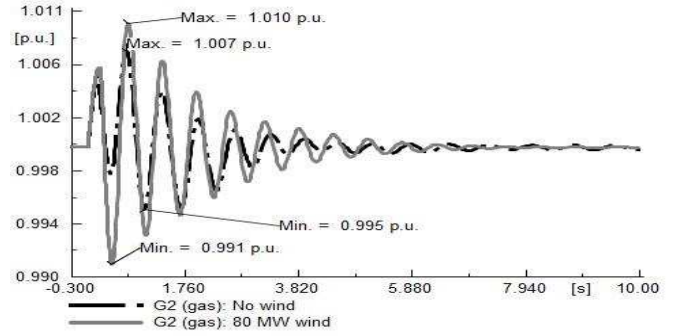


Fig. 12 Frequency of generator G2 with line outage

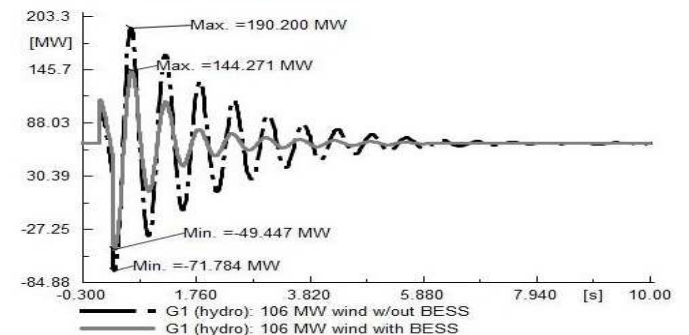
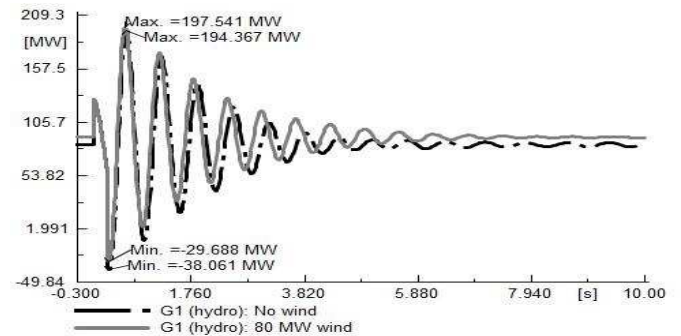


Fig. 13 Active power output of generator G1 with line outage

The lower minimum d-axis and q-axis value is selected to demonstrate the design or battery energy management flexibility for positive and negative frequency deviation. Battery SOC as shown in Fig. 16 remains nearly of the same value as before the incident and ready for next incident to respond.

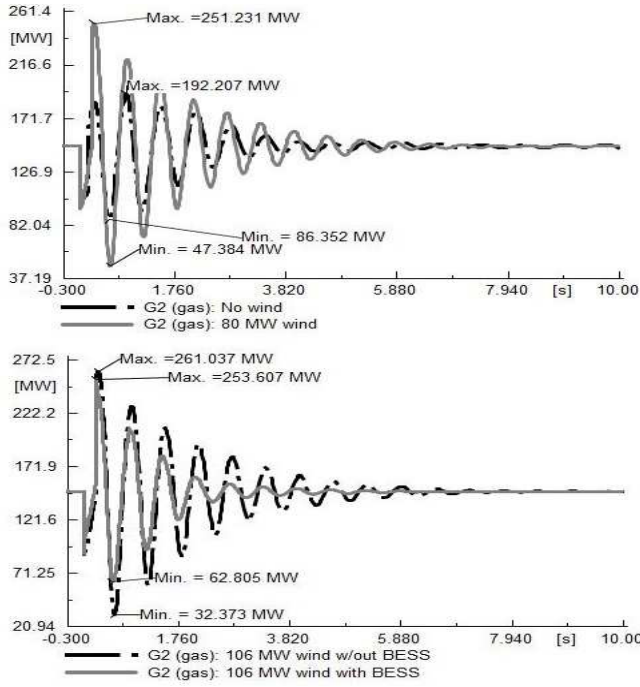


Fig. 14 Active power output of generator G2 with line outage

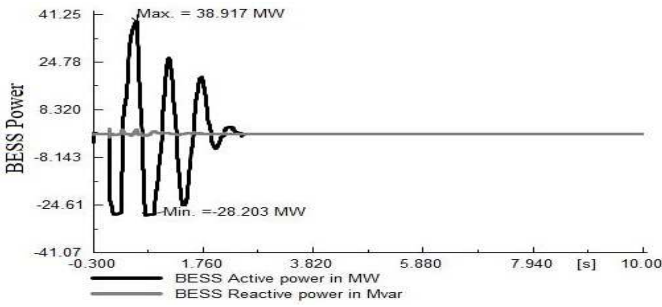


Fig. 15 BESS active/reactive power

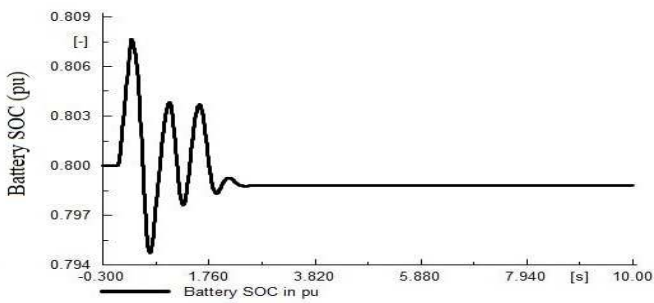


Fig. 16 Battery SOC

5.3. Case study-3: DG penetration and increase in load demand at load B

In order to further investigate BESS performance in stability enhancement, a sudden load increment and its impact on wind penetration limit is examined. With 120 MW wind power penetration, the systems capability to handle the amount of load demand increment is investigated. A 50% load increases at the highest load point of Load A is applied for the

duration of 1-1.5s and frequency response of the system is observed. Simulation results in Fig. 17 show that with 17.91% wind penetration and without a BESS, the system fails to handle efficiently 50% sudden load upsurge according to grid code requirement.

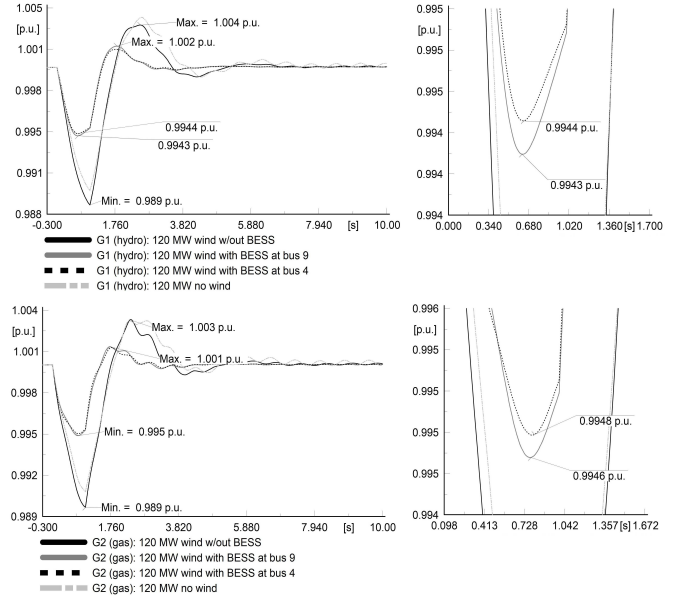


Fig. 17 The frequency of generators G1 and G2 with temporary load growth

The frequency drops to a value of 0.989 p.u which travels out of the mandatory $\pm 1\%$ of nominal value. However, without wind penetration, the system effectively maintains grid frequency oscillations within the allowed frequency corridor. This clearly defines the adverse inertia impact of wind energy. On the contrary, with the support of BESS, 50% load upsurge is possible to handle by the system when wind penetration is 17.91%. BESS is used to uphold frequency drop lower than the permissible limit. BESS is installed at two different locations in the network. It can be seen in Fig. 17 that when BESS is installed at swing generator (bus 4), the lowest frequency drop of G1 (0.9944pu) is slightly better than when BESS is installed at wind integrated bus (0.9943pu). A similar level of moderately improved performance is visible in the case of G2 when BESS is installed at bus 4.

BESS also minimizes active power oscillations that arise due to load demand changing circumstance. The BESS active power is shown in Fig. 18 that illustrates quite similar performance when BESS is installed at buses 4 and 9 and therefore a very similar level of SOC is visible for both locations as shown in Fig. 19. BESS provides the necessary power to reduce the drop in frequency value during the load growth periods. Since system frequency recovers to the nominal value at approximately 2.8s, BESS active power reduces to zero. Battery SOC goes down to a value higher than the previous cases as it provided large energy. However, steady-state battery SOC is nearly 0.77 pu at the end of the simulation that depicts BESS is capable to participate in any future event. If the SOC drops to the minimum value or to a

value that the BESS operator desires to charge, it is possible to charge the battery during the BESS inactive periods.

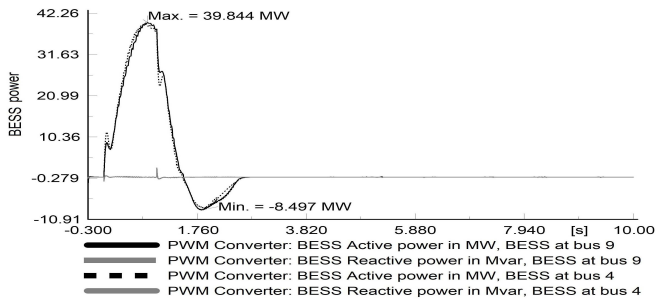


Fig. 18 BESS active/reactive power

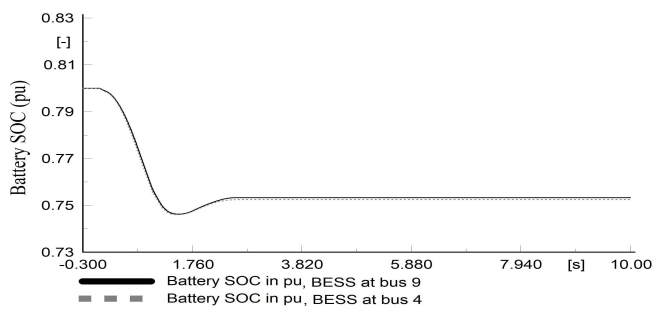


Fig. 19 Battery SOC

5.4. Case study-4: DFIGs and BESS in 39 Bus New England System

To further investigate the BESS performance, a large test system is considered with increased wind energy penetration. Total 4 wind farms (WFs) are integrated in the network and they are WF1 at bus 25, WF2 at bus 4, WF3 at bus 34 and WF4 at bus 16 as shown in Fig. 20. The rated power output of WF1, WF2 and WF4 is 300MW each and WF3 is 150MW. A permanent line outage event is applied on line 5-6 (marked in red cloud) at $t=1s$ following the clearance of line fault.

Simulation results of the impact of permanent line outage on system frequency are shown in Fig. 21. The impact of increased penetration of lower inertial DFIG is visible in the network performance. Following the permanent network event, 1050MW wind penetrated system (Wind-no BESS) shows higher frequency oscillations (1.0053pu) compared to no wind case (1.0003pu) that clearly illustrates the inertial impact of DFIG in the grid. Nevertheless, a 40MW BESS installed at bus 14 demonstrates lower frequency oscillation (1.0043pu) than the case without any BESS with the integrated wind (Wind-no BESS). In addition to lower frequency oscillation, Wind-BESS achieves moderately better steady-state frequency (1.0034pu) compared to Wind-no BESS condition (1.0036pu).

BESS active and reactive power is shown in Fig. 22 that illustrates BESS power consumption during the grid frequency higher than the BESS deadband. In this study, minimum active

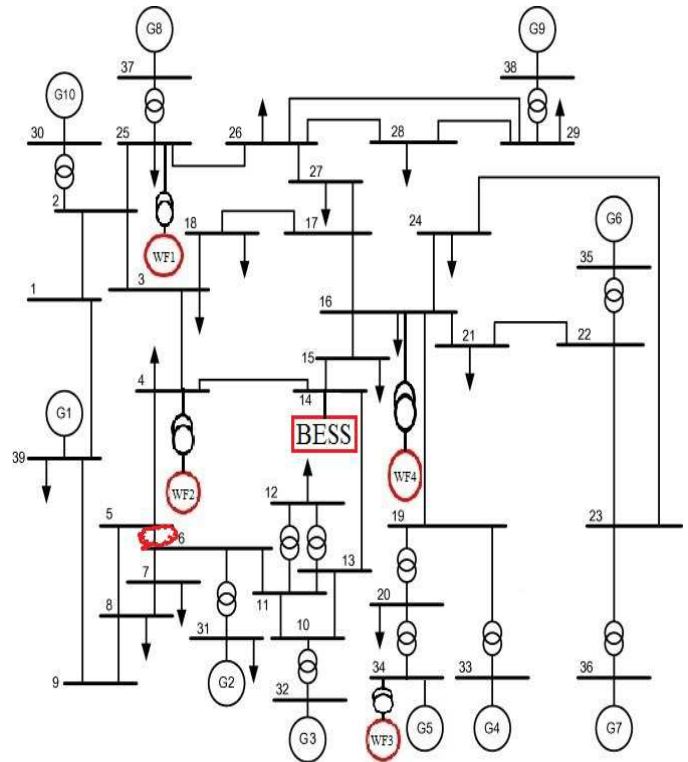


Fig. 20 New England 39 bus test system

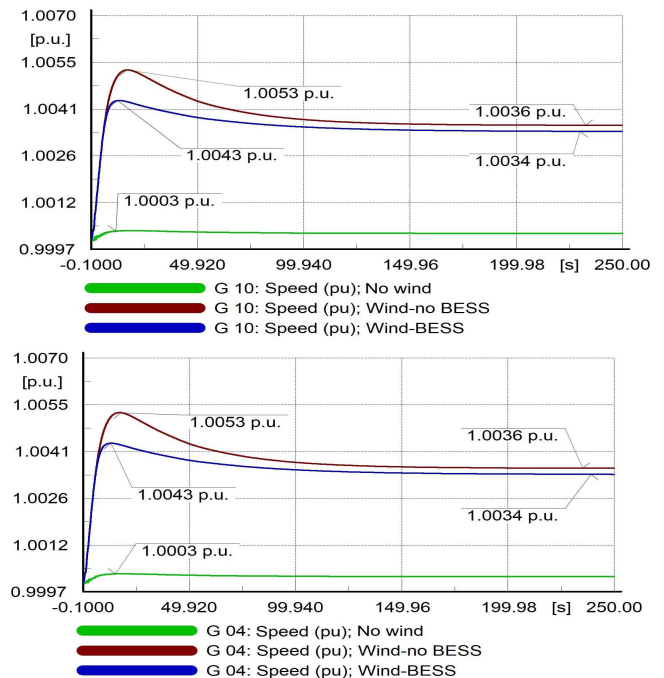


Fig. 21 The frequency of generators G10 and G4 with permanent line outage

current limit in d-axis is used as -1pu and therefore, BESS consumes 40MW during the over-frequency periods. Since the grid frequency is beyond the BESS deadband limit (0.003), BESS continues to consume the surplus energy. Battery SOC gradually increases as the battery continues to consume surplus energy as shown in Fig. 23. In consideration of BESS

operation for longer periods, BESS capacity plays the vital role and the selected battery rating is 12kAh. It is worth noting that this is not an optimal BESS energy capacity.

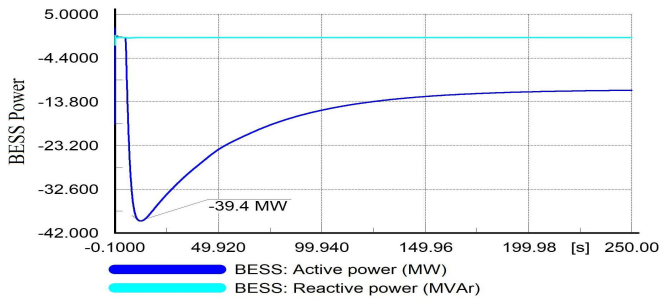


Fig. 22 Battery active/reactive power

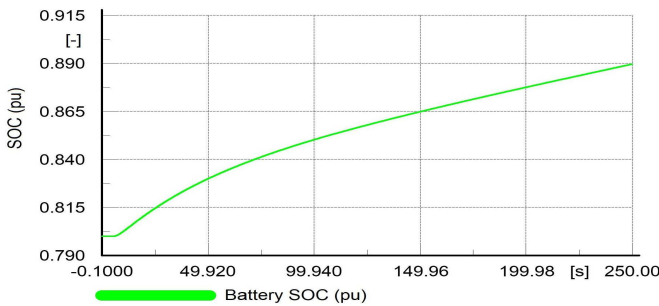


Fig. 23 Battery SOC

6. Conclusion

The BESS, as a quick responsive and reliable technology, have a remarkable prospect in regulating system frequency, particularly with large-scale penetration of intermittent RES. The limit of RES penetration level is constrained by the type of disturbance event and location. With increased wind penetration, accessible system inertia decreases and therefore system oscillation increases in the case of a disturbance event. Few types of research have studied the improvement of DG penetration. This study provides an extensive investigation on BESS contribution to reduce frequency oscillation, enhance system stability and facilitate the higher level of DG penetration.

Three different types of disturbances are applied and system responses are inspected. It is observed that with the increased penetration of wind energy, the system encounters various difficulties to maintain grid defined grid stability criteria. The incorporated BESS justifies its relevance in the power system to enhance frequency stability with increased wind energy penetration. BESS reduces frequency oscillation by absorbing excess energy and supplying energy deficit. BESS also minimises active power oscillation and the settling time of SGs in the system. It is also observed that wind energy penetration level is increased by 3.58-5.21% with the use of BESS. This indicates that high power but small energy BESS

capacity is imperative in ensuring improved primary frequency control of the system.

With the focus in a sustainable energy-oriented electricity industry, this proposed study of BESS contribution in facilitating increased DG penetration can potentially offer ample benefit to incorporate more clean energy sources with no reliability concern. The study provides a close insight into BESS importance in a future electric grid with 100% renewable energy penetration. Wind farm contribution in oscillation damping is not considered in this study. However, this can be included using power oscillation damper or pitch angle controller. Comparative technical and economic benefits of utilizing oscillation damping from the wind farm and BESS incorporation would be interesting.

Appendix A

Frequency controller: deadband- 0.0004, droop setting: $R=0.001$ Voltage controller: deadband- 0.1, droop setting: $R=1$ P controller: $K_p=1, K_i=1, T_{ip}=0.04, y_{min}=i_{d-min}=i_{q-min}=-0.7pu$ Q controller: $K_p=0.25, K_i=0.25, T_{iq}=1, y_{max}=i_{d-max}=i_{q-max}=1pu$, Current controller: $K_d=K_q=K_{id}=K_{iq}=1, T_d=T_q=0.01$ Battery parameter: Initial SOC=80%, Capacity/Cell (Ah)=12, no. of parallel cell=20, nominal voltage=0.9kV, $SOC_{min}=0.2, SOC_{max}=1$.

Conflicts of interest: None

This research is supported by the Victoria University under Research Training Program.

References

- [1] M.F. Akorede, H. Hizam, E. Poursmaeil, Distributed energy resources and benefits to the environment. *Renew. Sustain. Energy Rev.* 14 (2010) 724-734, <https://doi.org/10.1016/j.rser.2009.10.025>.
- [2] H. Polinder, J.A.Ferreira, B.B. Jensen, A.B.Abrahamson, K. Atallah R.A. McMahon. Trends in Wind Turbine Generator Systems, *IEEE Journal of Emerging and Selected Topics in Power Electronics* 3 (2013) 174-185, 10.1109/JESTPE.2013.2280428.
- [3] S. Bu, W. Du, H. Wang, Model validation of DFIGs for power system oscillation stability analysis, *IET Renew. Power Gener.* 11 (2017) 858-866, 10.1049/iet-rpg.2016.0980.
- [4] M.Q. Duong, N.T.N., Tran, G.N. Sava, M. Scripcariu, The impacts of distributed generation penetration into the power system. In: *Proceedings of Int. Conf. on Electromechanical and Power Systems (SIELMEN) 2017*. p. 295-301, 10.1109/SIELMEN.2017.8123336.
- [5] D.O. Ampofo, I.K. Othere, E.A. Frimpong, An investigative study on penetration limits of distributed generation on distribution networks, *Proceedings of IEEE PES PowerAfrica 2017*. p. 573-576, 10.1109/PowerAfrica.2017.7991289.
- [6] R. Sharma, M. Singh, D.K. Jain, Power system stability analysis with large penetration of distributed generation. *Proceedings of 6th IEEE Power India Int. Conf. (PIICON) 2014*. p. 1-6, 10.1109/POWERI.2014.7117685.
- [7] M.F.M. Arani, E.F. El-Saadany, Implementing Virtual Inertia in DFIG-Based Wind Power Generation, *IEEE Trans. on Power Syst.* 28 (2013) 1373-1384, 10.1109/TPWRS.2012.2207972.
- [8] L. Wu, D.G. Infield, Towards an Assessment of Power System Frequency Support From Wind Plant Modeling Aggregate Inertial Response, *IEEE Trans. on Power Syst.* 28 (2013) 2283-2291, 10.1109/TPWRS.2012.2236365.

- [9] M.F.M. Arani, Y.A.R.I Mohamed, Analysis and Impacts of Implementing Droop Control in DFIG-Based Wind Turbines on Microgrid/Weak-Grid Stability, *IEEE Trans. on Power Syst.* 30 (2015) 385-396, 10.1109/TPWRS.2014.2321287.
- [10] S. Wang, Y. Daren, Y. Jila, A coordinated dispatching strategy for wind power rapid ramp events in power systems with high wind power penetration, *International Journal of Electrical Power & Energy Systems* 64(2015) 986-995, <https://doi.org/10.1016/j.ijepes.2014.08.019>.
- [11] T. Surinkaew, I. Ngamroo, Hierarchical Co-Ordinated Wide Area and Local Controls of DFIG Wind Turbine and PSS for Robust Power Oscillation Damping, *IEEE Trans. on Sust. Energy* 7 (2016) 943-955, 10.1109/TSTE.2015.2508558.
- [12] A. Zertek, G. Verbic, M.A. Pantos, Novel Strategy for Variable-Speed Wind Turbines' Participation in Primary Frequency Control, *IEEE Trans. on Sust. Energy* 3 (2012) 791-799, 10.1109/TSTE.2012.2199773.
- [13] M. Fazeli, G.M. Asher, C. Klumpner, L. Yao, Novel Integration of DFIG-Based Wind Generators Within Microgrids, *IEEE Trans. on Energy Conversion* 26 (2011) 840-850, 10.1109/TEC.2011.2146253.
- [14] A.B. Attya, S. Ademi, M. Jovanovi, O.A. Lara, Frequency support using doubly fed induction and reluctance wind turbine generators, *Int. Journal of Electrical Power & Energy Systems* 101 (2018) 403-414, <https://doi.org/10.1016/j.ijepes.2018.04.007>.
- [15] A. Teninge, C. Jecu, D. Roye, Contribution to frequency control through wind turbine inertial energy Storage, *IET Renew. Power Gen.* 3 (2009) 358370, 10.1049/iet-rpg.2008.0078.
- [16] V. Courtecuisse, M.E. Mokadem, C. Saudemont, B. Robyns, J. Deuse, Experiment of a wind generator participation to frequency control, In: *Proceedings of Wind Power to the GridEPE Wind Energy Chapter 1st Seminar*, 2008 p. 1-6, 10.1109/EPEWECS.2008.4497317.
- [17] Y. Wang, J. Meng, X. Zhang, L. Xu, Control of PMSG-Based Wind Turbines for System Inertial Response and Power Oscillation Damping, *IEEE Trans. on Sustainable Energy* 6 (2015) 565-574, 10.1109/TSTE.2015.2394363.
- [18] R.H. Leon, D. Siguenza, D., Sanchez, J. Len, P.J. Ruiz, J. Wu, D. Ortiz, A survey of battery energy storage system (BESS), applications and environmental impacts in power systems, *Proceedings of IEEE Second Ecuador Technical Chapters Meeting*; 2017. p. 1-6, 10.1109/ETCM.2017.8247485.
- [19] I. Serban, R. Teodorescu, C. Marinescu, Energy storage systems impact on the short-term frequency stability of distributed autonomous microgrids, an analysis using aggregate models, *IET Renew. Power Gen.* 7 (2013) 531-539, 10.1049/iet-rpg.2011.0283.
- [20] Y. Wang, T. Phung, J. Ravishankar, Impact of battery storage on micro-grid transient performance, *Proceedings of IEEE Region 10 Conference* 2014. p. 1-6, 10.1109/TENCON.2014.7022448.
- [21] A.K. Srivastava, A.A. Kumar, N.N. Schulz, Impact of Distributed Generations With Energy Storage Devices on the Electric Grid, *IEEE Systems Journal* 6 (2012) 110-117, 10.1109/JSYST.2011.2163013.
- [22] Srivastava, A. K., Zamora, R., Bowman, D. Impact of distributed generation with storage on electric grid stability, In: *Proceedings of IEEE Power and Energy Society General Meeting* 2011 p. 1-5, 10.1109/PES.2011.6038923.
- [23] J. Fleer, P. Stenzel, Impact analysis of different operation strategies for battery energy storage systems providing primary control reserve, *Journal of Energy Storage*, 8 (2016) 320-338, <https://doi.org/10.1016/j.est.2016.02.003>.
- [24] P. Stenzel, J.C. Koj, A. Schreiber, W. Hennings, P. Zapp, Primary control provided by large-scale battery energy storage systems or fossil power plants in Germany and related environmental impacts, *Journal of Energy Storage* 8 (2016) 300-310, <https://doi.org/10.1016/j.est.2015.12.006>.
- [25] AEMC. The Frequency Operating Standard stage one final for-publi, [Online]<https://www.aemc.gov.au/sites/default/files/content/ce48ba94-b3a9-4991-9ef9-e05814a78526/REL0065-Review-of-the-Frequency-Operating-Standard-Final-for-publi.pdf>, [Accessed on: 2018-10-15].
- [26] M.K. Donnelly, J.E. Dagle, D.J. Trudnowski, G.J. Rogers, Impacts of the distributed utility on transmission system stability, *IEEE Trans. on Power Syst.* 11 (1996) 741746, 10.1109/59.496148.
- [27] J. Morren, J. Pierik, S.W.H.D. Haan, Inertial response of variable speed wind turbines, *Electric Power Systems Research* 76 (2006) 980-987, <https://doi.org/10.1016/j.epsr.2005.12.002>.
- [28] P.V. Brogan, R. Best, D.J. Morrow, C. Bradley, M. Rafferty, M. Kubik, Triggering BESS Inertial Response with Synchronous Machine Measurements, 2018 IEEE Power & Energy Society General Meeting (PESGM), Portland, OR, USA, 2018, pp. 1-5, 10.1109/PESGM.2018.8586499.
- [29] C. Zhou, K. Qian, M. Allan, W. Zhou, Modeling of the Cost of EV Battery Wear Due to V2G Application in Power Systems, *IEEE Trans. on Energy Conversion* 26 (2011) 1041-1050, 10.1109/TEC.2011.2159977.
- [30] M. Murnane, A. Ghazel, A Closer Look at State of Charge (SOC) and State of Health (SOH) Estimation Techniques for Batteries, [Online]<https://www.analog.com/media/en/technical-documentation/technical-articles/A-Closer-Look-at-State-Of-Charge-and-State-Health-Estimation-Techniques.pdf>.
- [31] H. Bitaraf, S. Rahman, M. Pipattanasomporn, Sizing Energy Storage to Mitigate Wind Power Forecast Error Impacts by Signal Processing Techniques, *IEEE Trans. on Sust. Energy* 6 (2015) 1457-1465, 10.1109/TSTE.2015.2449076.
- [32] P. Shen, M. Ouyang, L. Lu, J. Li, X. Feng, The Co-estimation of State of Charge, State of Health, and State of Function for Lithium-Ion Batteries in Electric Vehicles, *IEEE Trans. on Vehicular Tech.* 67 (2018) 92-103, 10.1109/TVT.2017.2751613.
- [33] Q. Xu, J. Xiao, P. Wang, X. Pan, C. Wen, A Decentralized Control Strategy for Autonomous Transient Power Sharing and State-of-Charge Recovery in Hybrid Energy Storage Systems, *IEEE Trans. on Sust. Energy* 8 (2017) 1443-1452, 10.1109/TSTE.2017.2688391.
- [34] PowerFactory, DIgSILENT, Application Example, 2017
- [35] Test Case P.M. Anderson Power System Introduction, <http://fglongatt.org/OLD/Test.Case.Anderson.html>, Accessed 16 January 2018
- [36] PowerFactory, DIgSILENT, 2017:SP2
- [37] D. PowerFactory, DFIG Template, (DigSILENT GmbH, 2017)